

Numerical Investigation of a Refractive Index SPR D-Type Optical Fiber Sensor Using COMSOL Multiphysics

D. F. SANTOS^{1,3}, A. GUERREIRO^{2,3}, and J. M. BAPTISTA^{1,3*}

¹*Centro de Ciências Exatas e da Engenharia, Universidade da Madeira, Funchal, Portugal*

²*Faculdade de Ciências da Universidade do Porto, Portugal*

³*INESC TEC, Porto, Portugal*

*Corresponding author: J. M. BAPTISTA E-mail: jmb@uma.pt

Abstract: Recently, many programs have been developed for simulation or analysis of the different parameters of light propagation in optical fibers, either for sensing or for communication purposes. In this paper, it is shown the COMSOL Multiphysics as a fairly robust and simple program, due to the existence of a graphical environment, to perform simulations with good accuracy. Results are compared with other simulation analysis, focusing on the surface plasmon resonance (SPR) phenomena for refractive index sensing in a D-type optical fiber, where the characteristics of the material layers, in terms of the type and thickness, and the residual fiber cladding thickness are optimized.

Keywords: Refractive index sensor, optical fiber sensor, surface plasmon resonance, light propagation simulation, COMSOL Multiphysics, graphical environment

Citation: D. F. SANTOS, A. GUERREIRO, and J. M. BAPTISTA, “Numerical Investigation of a Refractive Index SPR D-Type Optical Fiber Sensor Using COMSOL Multiphysics,” *Photonic Sensors*, vol. 3, no. 1, pp. 61–66, 2013.

1. Introduction

To estimate the behavior of an optical fiber sensor, it is very important to use a simulation tool to analyze parameters such as: magnetic and electric field intensities, effective refractive index, among others. Several difficulties exist in developing a good simulation program, including the necessary approximations when writing the code for 2D or 3D [1]. In particular, when the sensor structure is complex, the calculation becomes too cumbersome, and it is necessary to use simplified methods, for example: expansion and propagation method (MEP) and the method for multilayer structure transfer matrix modeling [2–3]. The latter allows a better approximation to the optical fiber cylindrical structure [4], but fails to get good results for

nano-structures in optical fibers [1]. One solution is to use finite-difference time domain (FDTD), which allows computing the magnetic and electric field distribution, but requires huge quantity of computing memory [5]. In this paper, we demonstrate another method of studying the behavior of optical fiber sensors based on the surface plasmon resonance (SPR) using COMSOL Multiphysics, a commercial program that uses finite element method (FEM).

On the other hand, D-type fiber is an optical fiber with numerous applications in optical sensing for different areas of engineering. Gas detection [6] and curvature sensing [7] are examples of sensing applications using this fiber. The D-type fiber has also been implemented as a biosensor using the surface-plasmon resonance technology [8, 9]. In this

simulation work, we improved the design of an SPR refractive index sensor, based on a D-type optical fiber, where the characteristics of the material layers, in terms of type and thickness, and the residual fiber cladding thickness were optimized.

2. Theory

We have analyzed an optical fiber sensor based on SPR composed by a D-type fiber spliced between two single mode fibers, as shown in Fig. 1. The main design parameters of the sensor included the length of the sensor L , the radius and refractive index of the core (r_c and n_c , respectively) and of the cladding (r_{cladd} and n_{cladd} , respectively), the distance between the core and the metal d (the residual cladding), the thickness of the metal d_m , and the refractive index of the external medium n_{ext} .

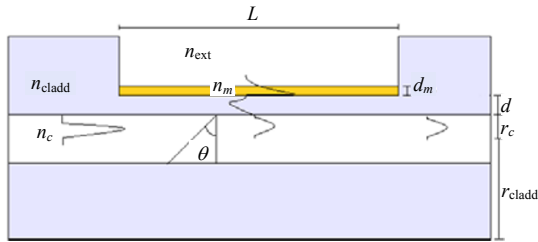


Fig. 1 Typical structure and behavior of a D-type fiber optic sensor based on SPR.

The losses of the light propagating in the fiber were determined by the tuning between the wavelength of the light beam and the SPR which was strongly dependent on the refractive index of the external medium. The transmission coefficient of the sensor could be used to assess with accuracy the value of n_{ext} .

2.1 Calculated transmission coefficient using COMSOL

In this work, we have conducted a 2D analysis of the mode structure and the electromagnetic field modes along the transverse plane of a D-type fiber using the mode analysis utilities of COMSOL Multiphysics. The electromagnetic fields in optical fiber waveguides are governed by the macroscopic Maxwell's equations in the absence of currents or external electric charges:

$$\nabla \times \mathbf{E}(r, t) = -\frac{\partial \mathbf{B}(r, t)}{\partial t} \quad (1)$$

$$\nabla \times \mathbf{H}(r, t) = \mathbf{J}(r, t) + \frac{\partial \mathbf{D}(r, t)}{\partial t} \quad (2)$$

$$\nabla \cdot \mathbf{D}(r, t) = \rho \mathbf{B}(r, t) \quad (3)$$

$$\nabla \cdot \mathbf{B}(r, t) = 0 \quad (4)$$

where \mathbf{E} , \mathbf{H} , \mathbf{D} and \mathbf{B} are the electric, the magnetic, the dielectric and the magnetic induction fields, respectively. Also, the term \mathbf{J} is the current density, ρ is the charge density, \mathbf{r} is the spatial coordinate, and t denotes time. The time-harmonic solutions describing strictly monochromatic fields are of the form

$$\mathbf{E}(r, t) = \mathbf{E}(r, \omega) e^{-j\omega t} \quad (5)$$

$$\mathbf{H}(r, t) = \mathbf{H}(r, \omega) e^{-j\omega t} \quad (6)$$

where ω is the angular frequency of light. In this representation, the fields are complex quantities whose real parts correspond to the physical fields [10].

In linear, isotropic, and nonmagnetic media, the following constitutive relations are

$$\mathbf{D}(r, t) = \varepsilon_0 \varepsilon_r \mathbf{E}(r, \omega) e^{-j\omega t} \quad (7)$$

$$\mathbf{B}(r, t) = \mu_0 \mathbf{H}(r, \omega) e^{-j\omega t} \quad (8)$$

where ε_0 and μ_0 are the permittivity and permeability of free space, respectively, and ε_r denotes the relative, material-dependent permittivity. In general, these quantities are functions of the spatial coordinates. Taking the curl of (1) and using (3), (7) and (8) yields the wave equation for the Fourier components electric field [10]:

$$\nabla \times (\nabla \times \mathbf{E}(r, \omega) - k_0^2 [\tilde{\varepsilon}_r(r, \omega)] \mathbf{E}(r, \omega)) = 0 \quad (9)$$

the same is the magnetic field:

$$\nabla \times [\tilde{\varepsilon}_r(r, \omega)]^{-1} \nabla \times \mathbf{H}(r, \omega) - k_0^2 \mathbf{H}(r, \omega) = 0 \quad (10)$$

where $c = \sqrt{\varepsilon_0 \mu_0}$ is the speed of light, and $k_0 = \omega c^{-1}$ is the wave number of the mode of the field. The term $\tilde{\varepsilon}_r(r, \omega) = \varepsilon_r(r, \omega) - j\sigma(r, \omega)/\omega\varepsilon_0$ represents the complex relative dielectric function written in terms of the material-dependent (real valued) relative permittivity ε_r and the Ohmic conductivity of the material $\sigma(r, \omega)$.

In optical fibers, the dependency in the spatial z coordinate along the axis is obtained using the variable separation method:

$$E_i(r, \omega) = E_i(r_{\perp}, \omega) e^{-j\omega\beta_i z} \quad (11)$$

$$H_i(r, \omega) = H_i(r_{\perp}, \omega) e^{-j\omega\beta_i z} \quad (12)$$

where β_i is the propagation constant of the i -th mode, and r_{\perp} is the position vector in the plane perpendicular to the optical axis. The solutions of (9) and (10) were obtained using the FEM, which basically consists in dividing the simulation domain into smaller subdomains forming a mesh as shown in Fig. 2. The subdomains have different sizes and are smaller near the interfaces between different media to account for steeper variations of the field. The field equations are then discretized into an algebraic system of equations and solved for their characteristic eigenvalues.

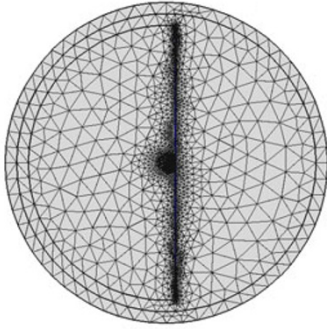


Fig. 2 Structure of the finite elements in COMSOL Multiphysics for a D-type optical fiber with a metallic layer for SPR.

The electric and magnetic fields are dependent on the angular frequency [(9) and (10)] as well as on the refractive index of the materials. For that, it is necessary to calculate the material's refractive index for all frequencies under study. For a dielectric layer, in this case of an optical fiber, it is possible to use the Sellmeier equation [3]

$$n^2(\lambda) = 1 + \sum_{q=1}^3 \frac{B_q \lambda^2}{\lambda^2 - C_q} \quad (13)$$

where B_q , C_q are the Sellmeier coefficients, determined experimentally [11], for a germanium-doped silica core fiber and fluorine-doped silica cladding. For the metallic layer, the permittivity and the refractive index can be obtained from the Drude model as

$$\varepsilon_m(\lambda) = 1 - \frac{\lambda^2 \lambda_c}{\lambda^2 (\lambda_c + j\lambda)} \quad (14)$$

$$n_m(\lambda) + jk_m(\lambda) = \sqrt{\varepsilon_m(\lambda)} \quad (15)$$

where n_m and k_m are the real and imaginary values of the refractive index for the metal, respectively, ε_m is the permittivity complex metal, and λ_c and λ_p denote the plasma wavelength and the collision wavelength, respectively, that is defined in [3] for the metals Ag, Au, Cu and Al.

Figure 3 illustrates the intensity of the electric field using the study "Mode Analyses" from COMSOL Multiphysics, for the structure of Fig. 1 and the mesh of Fig. 2 with [Fig. 3(a)] and without [Fig. 3(b)] a metallic layer, in this case of a 65-nm-thickness gold layer. The wavelength of the light was 802 nm. The study allowed confirming the single-mode behavior propagation in the optical fiber.

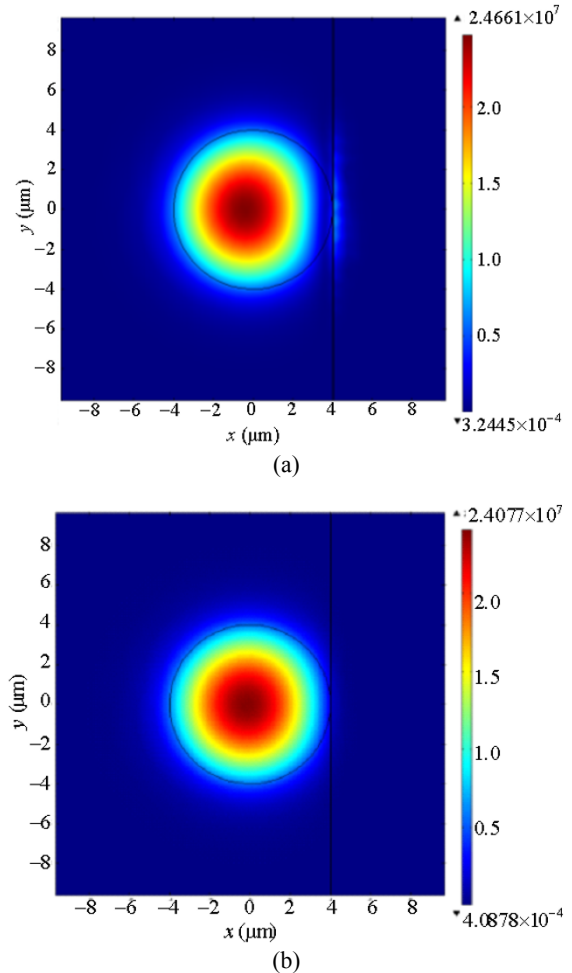
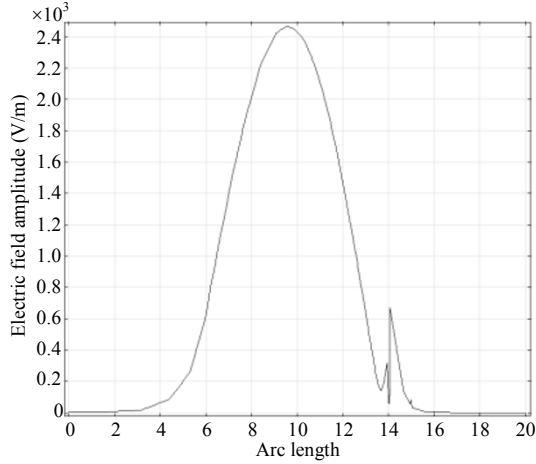
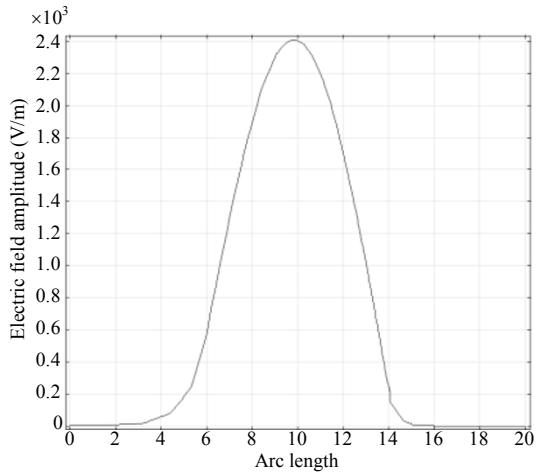


Fig. 3 Electric field distribution 2D near the fiber core for $\lambda=802$ nm (a) with the metal (Au) with a thickness of 65 nm and (b) without the metal.

The 1D electrical field amplitude in the optical fiber is also shown in Figs.4(a) and 4(b), with and without a metallic layer, respectively. Comparing both figures, it is possible to see the electric field intensity external to the fiber is stronger when using the metal.



(a)



(b)

Fig. 4 Electric field amplitude 1D across the fiber core for $\lambda=802$ nm (a) with the metal (Au) with a thickness of 65 nm and (b) without the metal.

Based on the simulation results provided by the COMSOL Multiphysics, one can compute the effective refractive index n_{eff} of the sensor [5] and from it the transmission coefficient T as a function of the wavelength λ , the external refractive index n_{ext} and the thickness of the metal d_m , according to the expression

$$T(\lambda, n_{\text{ext}}, d_m) = e^{-2n_{\text{eff}}(\lambda, n_{\text{ext}}, d)k_0L}. \quad (16)$$

2.2 Transmission coefficient calculated using Fresnel laws

To verify that the method works properly, a comparison was made with the implemented algorithm in [12], which used Fresnel equations applied to the structure in Fig. 1, allowing the transmission intensity to be written (for four layers) as

$$T(\lambda, n_{\text{ext}}, d) = (r_{1234})^{L/r_c \tan \theta} \quad (17)$$

where r_{1234} is the reflective coefficient for four layers as written

$$r_{1234} = \frac{r_{12} + r_{234}e^{j2k_2d}}{1 + r_{12}r_{234}e^{j2k_2d}} \quad (18)$$

where the reflective coefficients for three layers and two layers are, respectively

$$r_{234} = \frac{r_{23} + r_{34}e^{j2k_3d}}{1 + r_{23}r_{34}e^{j2k_3d}} \quad (19)$$

$$r_{ij} = \frac{n_i^2/k_i - n_j^2/k_j}{n_i^2/k_i + n_j^2/k_j} \quad (20)$$

where k_i is the component of the wave vector of the interface of the two layers of the sensor in the direction z and is given as $k_i = k_0(n_i^2 - n_1 \sin^2 \theta)^{1/2}$, where n_1 , n_2 , n_3 and n_4 represent the refractive indices of the core, cladding, metal and the external test medium, respectively.

Applying (16) and (17), it is possible to obtain the results by the two different methods, as shown in Fig. 5. The behavior of the two methods was similar, having a difference between the transmission coefficients and a small shift in the wavelength dips. We attributed this difference to the fact that in the Fresnel equations' algorithm it is only considered planar waves in a fairly symmetrical arrangement. On the other hand, when using the FEM, we considered the D-type fiber as a non-symmetrical cylindrical waveguide, being able to model the inhomogeneous optical regions with a resolution of the cell size, resulting in a more accurate outcome. In terms of the results and in what concerns the material thickness, the optimal point occurred when a layer with a thickness of 55 nm to 65 nm was used.

Another way to test the efficiency of the described procedure is to calculate the sensor sensitivity (λ /RIU) as function of the different refractive indices of the external environment. The sensitivity for both methods is almost equal and is close to 3150nm/RIU [2].

Tailoring the simulation analysis in COMSOL Multiphysics, it is possible to optimize the sensitivity, transmission coefficient dip, wavelength operation area, amongst others for a refractive index SPR D-type optical fiber sensor. To decrease the depth of the transmission coefficient dip and consequently lower the sensitivity of the external medium, d can be increased, as shown in Fig. 6.

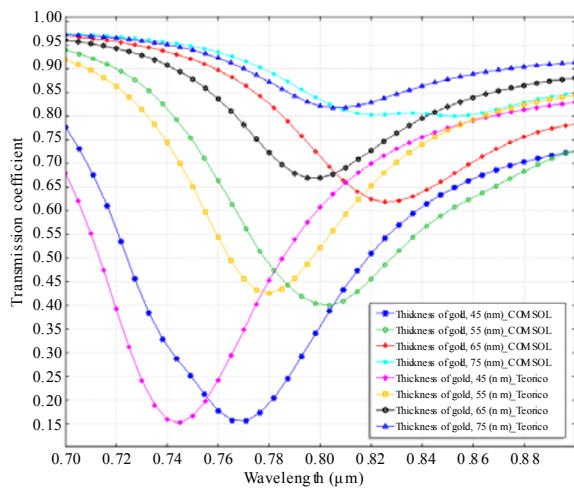


Fig. 5 Transmission coefficient T as a function of the wavelength and metallic layer thicknesses (Au), $d_m=0 \mu\text{m}$, $L=1 \text{mm}$, $n_{\text{ext}}=1.3943$ and $\theta=88.85^\circ$.

From Figs. 5 and 6, it is possible to have a sensor that works for an area of operation near 820nm, for a metal thickness of 65 nm (Au).

In case another wavelength is required, one possible solution is to apply an additional layer of a dielectric with a high refractive index, such as tantalum pentoxide (Ta_2O_5)[1–2], which simulation results can be seen in Fig. 7 and compared with the results presented in [2]. For different thicknesses of Ta_2O_5 , the transmission coefficient dip of the sensor operation is not significantly altered being possible to tailor the wavelength sensor operation [2].

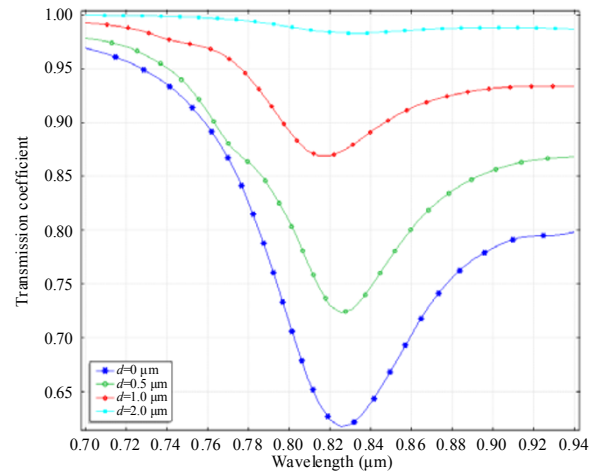


Fig. 6 Simulation of transmission coefficient of the sensor, for different cladding thicknesses: in this simulation, the thickness of the gold layer is 65 nm, and the refractive index of the external environment is 1.3934.

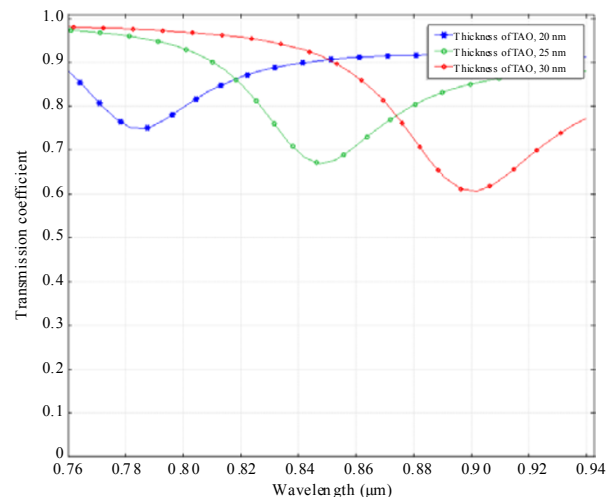


Fig. 7 Simulation of transmission coefficient T of the sensor for different thicknesses of the dielectric (Ta_2O_5): the thickness of the gold is 65 nm and $n_{\text{ext}}=1.329$.

3. Conclusions

Another method was demonstrated to study the behavior of optical fiber sensors for refractive index measurement based on SPR using COMSOL Multiphysics, a commercial program that uses the finite element method. The two simulations, one with COMSOL Multiphysics and the other with Fresnel’s equations, present a similar behavior. The graphical interface of COMSOL Multiphysics facilitates the simulation work, having no need to

develop complex formulations. Also, it has the ability to model inhomogeneous optical regions with a resolution of the cell size and allows the analysis of other parameters such as the intensity of magnetic and electric field across the structure [13]. COMSOL Multiphysics permits in a graphical environment more accurate and realistic results than traditional approaches, although at the expense of longer running time.

It was also possible to demonstrate the use of COMSOL Multiphysics to improve the performance of a refractive index SPR D-type optical fiber sensor, where the characteristics of the material layers, in terms of the type and thickness, and the residual fiber cladding thickness are optimized.

Open Access This article is distributed under the terms of the Creative Commons Attribution License which permits any use, distribution, and reproduction in any medium, provided the original author(s) and source are credited.

References

- [1] B. Lee, S. Roh, and J. Park, "Current status of micro- and nano-structured optical fiber sensors," *Optical Fiber Technology*, vol. 15, no. 3, pp. 209–221, 2009.
- [2] R. Slavik, J. Homola, J. Ctyroký, and E. Brynda, "Novel spectral fiber optic sensor based on surface plasmon resonance," *Sensors and Actuators B: Chemical*, vol. 74, no. 1–4, pp. 106–111, 2001.
- [3] A. K. Sharma and B. D. Gupta, "On the performance of different bimetallic combinations in surface plasmon resonance based fiber optic sensors," *Journal of Applied Physics*, vol. 101, no. 9, p. 093111-1–093111-6, 2007.
- [4] E. Anemogiannis, E. N. Glytsis, and T. K. Gaylord, "Transmission characteristics of long-period fiber gratings having arbitrary azimuthal/radial refractive index variations," *Journal of Lightwave Technology*, vol. 21, no. 1, pp. 218–227, 2003.
- [5] Y. Al-Qazwini, P. T. Arasu, and A. S. M. Noor, "Numerical investigation of the performance of an SPR-based optical fiber sensor in an aqueous environment using finite-difference time domain," in *Proc. 2011 2nd International Conference on Photonics*, Oct. 17–19, vol. 1, pp. 1–4, 2011.
- [6] B. Culshaw, F. Muhammad, R. Van Ewyk, G. Stewart, S. Murray, D. Pinchbeck, *et al.*, "Evanescent wave methane detection using optical fibers," *Electronics Letters*, vol. 28, no. 24, pp. 2232–2234, 1992.
- [7] F. M. Araújo, L. A. Ferreira, J. L. Santos, and F. Farahi, "Temperature and strain insensitive bending measurements with D-type fiber Bragg gratings," *Measurement Science and Technology*, vol. 12, no. 7, pp. 829–833, 2001.
- [8] M. H. Chiu, S. F. Wang, and R. S. Chang, "D-type fiber biosensor based on surface-plasmon resonance technology and heterodyne interferometry," *Optics Letters*, vol. 30, no. 3, pp. 233–235, 2005.
- [9] Y. Chen and H. Ming, "Review of surface plasmon resonance and localized surface plasmon resonance sensor," *Photonics Sensors*, vol. 2, no. 1, pp. 37–49, 2012.
- [10] M. Fliziani and F. Maradei, "Edge element analysis of complex configurations in presence of shields," *IEEE Transactions on Magnetics*, vol. 33, no. 2, pp. 1548–1551, 1997.
- [11] A. Méndez and T. F. Morse, *Specialty Optical Fibers Handbook*. San Diego, California: Academic Press, 2007, pp. 39–40.
- [12] M. H. Chiu, C. H. Shih, and M. H. Chi, "Optimum sensitivity of single-mode D-type optical fiber sensor in the intensity measurement," *Sensors and Actuators B: Chemical*, vol. 123, no. 2, pp. 1120–1124, 2007.
- [13] D. Christensen and D. Fowers, "Modeling SPR sensors with the finite-difference time-domain method," *Biosensors & Bioelectronics*, vol. 11, no. 6, pp. 677–684, 1996.